Iranian Journal of Chemistry and Chemical Engineering (IJCCE)

Preparation and Characterization of the Inter-Polymer Complexes between Poly (allylamine hydrochloride) and Poly(vinyl sulfonic acid) ~~Electron Donor and Electron Acceptor polymers~~

Amir Sepehrianazar[1*], Olgun Güven[2]

1) Department of Chemistry, Ahar Branch, Islamic Azad University, Ahar, Iran. Tel: 4144239781

2) Hacettepe University, Department of Chemistry, 06800 Beytepe, Ankara, Turkey

[*]Corresponding Author: Amir Sepehrianazar; E-mail: Amir.Sepehrianazar@iau.ac.ir

ORCID: 0000-0002-3855-2404

Abstract: *Poly (allylamine hydrochloride) P(AlAm.HCl) is a cationic polymer with many applications because of the existing amines group. Its importance becomes evident as poly (vinyl amine) polymer cannot be ~~produced~~ prepared from its monomer via free radical polymerization. Poly(vinyl sulfonic acid) P(VSA) is an anionic polymer with many applications, such as drug delivery and DNA modification. The synthesis of a new amphiphilic interpolymer complex (IPC) ~~production~~ was the aim of the study. Aqueous solutions of P(AlAm.HCl) and P(VSA.Na) were physically mixed in variant ~~monomer~~ repeating unit concentrations that yielded water-insoluble IPCs. FT-IR was used to identify the structures ~~behavior~~ of the IPCs, and TGA was used to determine their thermal properties. XRD patterns were performed to determine the strength of the IPCs. Strong interpolymer complexes were formed in the mole ratio (0.25:1) in feed compositions approved by XRD and TGA. Scanning electron microscopy (SEM), micrographs assessed the morphology of the IPC. ~~After removing acid from~~ IPC of deacidified P(AlAm.HCl), ~~a physical mixture of~~ and P(VSA) was prepared with different mole ratios of repeating units ~~monomers~~. These physical IPCs are water-soluble. FT-IR and ^{1}H-NMR were applied to examine the ~~obtained~~ formation of sulfonamide groups and the structural characterization of IPCs between P(AlAm) and P(VSA) at different molar ratios. ~~The sulfonamide group was obtained at 170°C per hour with a (1:1) molar ratio feed composition. However, a sulfonamide group was not evident even at high temperatures due to the salt in the mixture of P(AlAm.HCl) and P(VSA.Na).~~*

Keywords: *Poly(vinyl sulfonic acid); Poly(allylamine hydrochloride); Interpolymer complex polymer (IPC); TGA; XRD*

Introduction:

The interpolymer complex *(IPC)* is formed through the interaction of the physical structure of both electron donor and electron acceptor polymers. This physical structure can take various forms such as linear, block-graft copolymers, polymer brushes, stars, liposomes, and zwitterions. Different characteristics can be created from the baseline components by utilizing hydrogen bonds between donor-acceptor units and electrostatic interactions between polyanions and polycations functional groups. This opens up the possibility of developing various functional materials. [1-3] Recently, there has been a significant interest in studying the interactions between poly(zwitterions) and a range of chemicals, low molecular weight salts, charged polyelectrolytes, and proteins. Numerous projects have been undertaken to explore the characteristics of *IPCs*. [4-10] Particularly fascinating are the zwitterionic structures found in biopolymers. Synthetic poly(zwitterions) have the potential to produce biocompatible and non-immunogenic substances that can prevent protein destruction. [3,5] These properties make them valuable in modifying medical products and advancements in membrane structure technologies.

The studies by Kudaibergenov and Nuraje [11]; Kabanov and Zezin [12]; Wen *et al.* [13]; Ma *et al.* [14]; and Zucolotto *et al.* [15] contribute to the progressive development in inter-polyelectrolyte (or interpolymer) complexes *(IPC)*. The polyelectrolyte– polyelectrolyte complex's behavior has been recently reviewed. [16-20] Hydrogen-bonded *IPCs* are more considered in this point of view. [21, 22] Kabanov *et al.* conducted the initial investigation on the complexation of 2-methyl-5-vinylpyridine-acrylic acid *(2M5VPy-co-AA)* with poly(acrylic acid) *(PAA)*. [12] The ionic and hydrogen bonds between the *2M5VPy-co-AA* and *PAA* in the standard cooperative system have been demonstrated to play a crucial role in the formation of the polyelectrolyte-polyampholyte complex *(PPC)*. In recent decades, there has been a growing interest among researchers in solid polymer electrolytes *(SPE)*. [1, 2] These materials are high-quality composites called *SPEs*. They have ionic conductivity, high stability, high specific energy, and good mechanical and thermal properties. [2-4] In addition, the applications of different chemical devices, such as rechargeable batteries and electrochemical devices, have increased the importance of these materials. [5-7] *SPEs* generally have low electrical conductivity at controlled temperatures. We can increase the *SPEs'* electrical conductivity through various methods, such as *IPC* production and ionic or mineral fillers. [6, 8, 23] *IPC*

polymers are used in drug delivery, layer-by-layer film preparation [14-16], and *DNA* and *RNA* modification. [22-23] Units fashioned from polyelectrolyte complexes are created by combining oppositely charged polymers or macromolecules. [20-22]These complexes are formed through electrostatic interactions between the positively and negatively charged components, resulting in the formation of a stable structure. [24-27] Polyelectrolytes *(PEs)* with opposite charges are brought together by electrostatic forces, resulting in the formation of polyelectrolyte complexes *(PECs).* These complexes consist of hydrogen bonding structures, which are created by the combination of polymers that have units capable of accepting and donating protons. [27-34]The formation of stereo-complexes is predominantly driven by the attractive van der Waals forces, which give rise to a complex structure with a higher level of organization. [18-21] Charge-transfer complexes *(CTCs)* are formed within polymer systems that involve both electron-accepting and electron-donating components, resulting in charge-transfer interactions. [12-14]

IPCs are products of non-covalent interactions between complementary, unlike macromolecules in solutions. These complexes include *IPCs, PEs*, hydrogen bonding complexes *(HBC),* and *(CTCs)*. [30-34] *P(AlAm.HCl)* is a commonly encountered polycationic polymer known as polyallylamine hydrochloride. This particular polymer exhibits promising potential for various applications owing to the presence of amine groups within its molecular structure. [25]

Initially, *P(AlAm.HCl)* was synthesized through irradiation. However, a subsequent method for its synthesis involved the utilization of a radical initiator in a thermal process. The instability of poly(vinylamine) *(PVA),* an amine polymer, prevents its synthesis from the corresponding monomer. [25]

As a result, *P(AlAm),* the closest analog to *PVA,* is synthesized from its acid salts. This is primarily due to the challenges associated with allylic monomer polymerization. *P(AlAm)* is readily available in the market, but typically in low molecular weights. [25]

P(VSA) is considered the most basic form of polymeric monoprotic acid. In terms of its potential applications, the comparison between acrylic acid *P(AA)* and polyvinyl phosphonic acid reveals the extent of their usefulness and scope. [26] Despite extensive research, there remains a lack of comprehensive understanding regarding the intricacies involved in the

synthesis of this particular subject matter. [22-25] *P(VSA)* is a polymer that plays a vital role due to its sulfonic acid composition. This polymer possesses a notable benefit in the form of a substantial concentration of sulfonate groups. [26] The practical significance lies in the anionic polyelectrolyte interactions between *P(VSA)* derivatives and biomolecules. These interactions between negatively charged *P(VSA)* derivatives and biomolecules have practical implications and are of interest in various applications. [26, 32]

The scientific and industrial communities have shown a growing fascination with polyelectrolyte complexes, as reflected in the numerous articles published on this subject. [17-22]The classification of *PECs* involves categorizing them into two distinct groups: electron donors or acceptors, and a second group known as PE-surfactants *(PE-surfs)*. [17-18]

Polyelectrolyte-surfactant complexes *(PE-surfs)* encompass a combination of anionic polyelectrolytes, cationic surfactants, anionic surfactants, and ionic polyelectrolytes. [22-24, 27] An aqueous solution is created by mixing two species with opposite charges, namely polyelectrolyte-polyelectrolyte or polyelectrolyte-surfactant. Despite this, numerous methods have been devised to produce polyelectrolyte complexes *(PECs)* and polyelectrolyte surfactants *(PE surfs).* [17-22] According to the review of articles, there needs to be more detailed information about the physical formation and accurate structural identification of *P(AlAm.HCl)* and polyvinyl sulfonic acid sodium *P(VSA.Na)* salt polymers. [28, 30] In different monomer-based mole ratios, we prepared an *IPC* between *P(AlAm.HCl)* and *P(VSA.Na). FT-IR* and ^{1}*H-NMR* characterized the structural behavior of the *IPCs*, while *TGA*, *XRD*, and *SEM* were used to investigate the thermal properties and morphological behavior. Also, we prepared an *IPC* using deacidified *P(AlAm.HCl)* with *P(VSA)* and characterized by *FT-IR* and ^{1}*H-NMR*. The power of the acidified and deacidified complexes was compared using *XRD* and *TGA*. Furthermore, we investigated the thermal properties and morphology of the *IPC* by *TGA* and *XRD*.

Experimental:

Materials

In this study, ~~we used~~ Allylamine (98% pure Aldrich) ~~as a monomer~~ and 2,2'-azo-bis (2-methyl propanediamine) dihydrochloride (Aldrich) were used as the monomer and thermal initiator respectively. ~~as an~~ initiator. *AlAm* was complexed with 37% of 12*N HCl*. ~~The acid was procured~~

~~from the renowned Merck Company located in Darmstadt, Germany.~~ Additionally, precipitating substances like methanol, ethanol, and organic solvents were ~~also~~ obtained from the ~~same~~ Merck Company (Darmstadt, Germany). The monomer *(VSA.Na)* used in the experiment was acquired as a 25% aqueous solution from Aldrich. [25]

AlAm Salts Preparation

12*N HCl* solution was filled in three-necked containers, ~~which included~~ with an attached condenser and stirrer. The temperature of *AlAm* was lowered to a range of -10 to 0°C, and subsequently, *HCl* was added drop by drop to the *AlAm* solution while maintaining the temperature ~~of~~ around 5-10°C. This process resulted in the formation of a clear solution of ~~known as~~ *AlAm.HCl.* [25]

Polymerization of *AlAm.HCl* in Water

~~The~~ 6.68 *g* of 70 % *(AlAm.HCl)* solution was poured into a four-necked flask ~~container~~, including a nitrogen inlet, stirrer, thermometer, and reflux condenser.

The process began by adding an initiator solution, specifically 2,2'-azo-bis (2-methyl propanediamine) dihydrochloride, to 0.35 *mL* of water. This resulting solution was then combined with the monomer and stirred for a duration of ten hours at a temperature of 50°C. After the initial ten hours of stirring, the stirring ceased, and the polymerization process continued for an additional 40 hours. The resulting polymer was precipitated in ethanol, ~~resulting in~~ with the formation of a viscose and colorless compound. This precipitate was then filtered, washed, and subjected to extraction with ethanol in a soxhlet apparatus for a period of 15 hours, which equated to approximately 60 cycles. The purpose of this extraction was to remove any remaining unpolymerized monomer. Finally, the precipitate was dried in a vacuum owen at 50°C, resulting in the formation of a white powder ~~known~~ as poly(allyl ammonium) chloride. [25]

Deacidification of *P(AlAm.HCl)*

In the methanol suspension solution, we introduced 2.9 N sodium hydroxide *(NaOH)* to the *P(AlAm.HCl).* The suspension was allowed to stand for a duration of one hour, after which it was refrigerated overnight. The resulting precipitate of *NaCl* was separated by decanting and solution was subsequently evaporated until completely dry. [25, 27]

Polymerization of *VSA* in Water

A four-necked ~~container~~ flask equipped with a nitrogen inlet, stirrer, and reflux condenser was utilized to hold 6.68 g of a 25% *VSA* solution. The solution was subjected to deoxygenation by nitrogen purge and heated to a temperature of 50°C. Subsequently, a solution containing the ~~an~~ initiator, specifically 2,2'-azo-bis (2-methyl propanediamine) dihydrochloride, was prepared by dissolving it in 0.35 mL of water. This initiator solution was then added to the monomer. The resulting mixture was stirred for a duration of ten hours while maintaining the temperature at ~~of~~ 50°C. Following this, the stirring was halted, and the polymerization process was allowed to continue for an additional 40 hours. ~~As a result,~~ The polymer formed was precipitated in ethanol, yielding a colorless and viscous liquid product. ~~polymer~~. The precipitate was subsequently filtered, washed, and subjected to extraction with ethanol in a soxhlet apparatus for a period of 15 hours, which involved approximately 60 cycles. This extraction process aimed to eliminate any remaining unpolymerized monomer. Finally, the precipitate was dried under vacuum conditions at ~~a temperature of~~ 50°C, resulting in the formation of a white powder of *P(VSA)*. [26]

Preparation of Interpolymer Complexes

To create *IPCs* with varying repeating unit-based mole ratios using different concentrations of polymers. ~~monomers~~, Predetermined amounts of the salts of *P(AlAm.HCl)* and *P(VSA.Na)* were dissolved in water. The resulting solution containing both polymers was carefully mixed and then separated through precipitation using a filter. Subsequently, the ~~mixture~~ filtrate was subjected to vacuum at a temperature of 50°C for a duration of 24 hours.

Characterization of *IPCs*:

***FT-IR* Analyses**

FT-IR spectro~~photo~~meter (Nicolet 520 model U.S.A) was ~~applied~~ used for *FT-IR* analysis. The KBr discs were made for the samples. Spectra conditions were 64 scans ~~and~~ at 4 cm^{-1} resolution.

The *FT-IR* ~~spectroscopy~~ bands for *P(AlAm.HCl);*

3300-3500 (γNH_3^+), 2800-3000 (γCH_2), 1500-1700(NH_3^+ bending) 1000-1200 (NH_3^+ bending), 700-900((NH_3^+ bending). [25]

For *P(AlAm);*

3300 (γNH_2), 2800 (γCH_2), 1500-1600(NH_2 bending), 700-900(NH_2 bending), 1350-1450(CH bending). [25]

For *P(VSA.Na),* and *P(VSA);*

The spectrum displays several characteristic peaks at different wavenumbers. These include peaks at 1037 cm^{-1} and 1120 cm^{-1}, which correspond to the stretching vibrations of the sulfur-oxygen bond *($\gamma S=O$)*. Another peak is observed at 3500 cm^{-1}, indicating the presence of hydroxyl groups *(γO-H).* The range between 3000-2900 cm^{-1} shows peaks related to the stretching vibrations of carbon-hydrogen bonds *(γC-H_2).* Additionally, there are peaks at 1700 cm^{-1} (CH_2 bending), 1650 cm^{-1} (SO_2 bending), 1400 cm^{-1} (*CH* bending), 1200 cm^{-1} (*OH* bending), 1050 cm^{-1} (SO_2 bending), and 500-800 cm^{-1} (SO_2 bending). These peaks provide valuable information about the molecular structure and functional groups present in the compound. [25]

~~The *IPC* was prepared by dissolving and mixing *P(AlAm.HCl)* and *P(VSA.Na)* in water while continuously stirring. The resulting precipitant was then filtered, dried, and subsequently placed in a vacuum at a temperature of 50 ^oC for a duration of 24 hours. *FT-IR* analysis showed the peak intensities at 1650-2000 cm^{-1} and 3000 cm^{-1}. It is thought that peak intensities were increased with increasing the amount of *P(AlAm.HCl).*~~

***NMR* analyses**

A 0.01 *g* portion of the polymer sample was dissolved in 0.7 *mL* of deuterium oxide (D_2O), and subsequently, ~~a study using a~~ ^{1}*H-NMR* ~~technique~~ was conducted. The ^{1}*H-NMR* instrument employed for this study was the Bruker U.S.A Ultra Shield 400 *MHz NMR* spectrometer.

^{1}H-*NMR* peaks for *P(AlAm.HCl);*

0.9-1.2 *ppm* CH_2 polymerization grows allyl degradation, 1.2-1.6 *ppm* CH_2 main chain normal polymerization, 1.8-2.2 *ppm CH* main chain normal polymerization, 2.8-3.3 *ppm* CH_2 side chain normal polymerization, 3.5-3.7 CH_2 side chain polymerization grow allyl degradation. [25]

^{1}H-NMR for *P(AlAm);*

0.9-1.4 *ppm* CH_2 main chain polymerization, 1.4-1.7 *ppm CH* main chain polymerization, 2.4-3.1 *ppm* CH_2 side chain, 3.5-3.8 *ppm* NH_2. [25]

^{1}H-NMR for *P(VSA)*;

1.4-3.0 *ppm* CH_2 main chain, 3.0-4.0 *ppm CH* main chain, 5.4-6.2 *ppm OH*. [26]

^{1}H-NMR for *P(VSA.Na)*;

1.4-2.8 *ppm* CH_2 main chain, 3.0-4.0 *ppm CH* main chain, 5.4-6.2 *ppm OH*. [26]

^{1}H-NMR for *P(AlAm)-P(VSA)* (1:1) monomer repeating unit;

1.2-1.8 *ppm* CH_2 *AlAm* in the main chain, 1.8-3.0 *ppm* CH_2 main chain in *VSA*, 3.0-4.4 ppm CH main chain VSA, 2.4-3.0 *ppm* CH_2 side chain in *AlAm*, 1.4-1.7 *ppm CH* main chain in *AlAm*, 5.7-6.4 *ppm OH* in *VSA*

^{1}H-NMR for (1:0.25) monomer repeating unit;

1.2-1.8 *ppm* CH_2 *AlAm* main chain, 1.4-1.7 *ppm CH AlAm* main chain, 1.9-3.1 *ppm* CH_2 main chain *VSA*, 3.2-4.4 *ppm CH* main chain *VSA*, 2.5-3.0 *ppm* CH_2 side chain *AlAm*, 5.7-6.5 *ppm OH VSA*

^{1}H-NMR for (0.25:1) monomer repeating unit;

1.9-3.0 *ppm* CH_2 main chain *VSA*, 1.8-2.0 *ppm* CH_2 main chain *AlAm*, 1.4-1.7 *ppm AlAm*, 2.5-3.0 *ppm* CH_2 side chain *AlAm*, 3.0-4.0 *ppm CH* main chain *VSA*, 5.7-6.5 ppm OH VSA

Investigation of the Thermal Properties

IPC samples were characterized by conducting thermal gravimetric analysis (TGA) using a Perkin Elmer Pyris model thermogravimetric analyzer from the United States. The samples under investigation consisted of 5-10 mg of powders, which were subjected to TGA analysis. The nitrogen flow rate was maintained at 20 mL/min during the experiments. The weight loss as a function of temperature ~~ratio~~ was measured as the temperature varied from room temperature to 900 ℃ at a heating rate of 20 ℃/min. Subsequently, the collected data were subjected to analysis.

XRD Analysis

To assess the crystallinity of *IPC*, a Rigaku *D/Max* 2200 diffractometer from Japan was employed to analyze 10 mg of powder. The analysis encompassed the utilization of *CuKα (λ* =1.54059 *Å*) radiation and measured the angle *2Θ* while maintaining a temperature range of 0°C to 60°C.

SEM Analyses

The *XRD* analysis samples were subjected to a treatment involving the use of two milligrams of *IPC* powder, which was subsequently coated with gold using a vacuum evaporator. The morphologies of the *IPC* were then examined using a Jeol *JSM-6060LV* model Scanning Electron Microscope *(SEM)* from the U.S.A.

Result and Discussion:

P(AlAm.HCl) is cationic, and P(VSA) is an ionic polymer. These polymers, ~~besides~~ as well as their copolymers, were synthesized by Sepehrianazar *et al*. [25,27]. In this study, we investigate IPC formation between these two polymers.

Investigation of IPCs Structural behavior by FT-IR

To compare *AlAm.HCl/VSA* co-polymers and their *IPCs*, a mixture of different mole ratios of *P(AlAm.HCl)* and *P(VSA.Na)* were prepared in an aqueous solution to form an *IPC*. The resulting *IPC* was obtained by mixing *P(AlAm.HCl)* with *P(VSA.Na)*. The *FT-IR* spectra analysis revealed that the NH_2 stretching intensity and the amount of *AlAm* increased at 3100 cm^{-1}. Additionally, the bending intensity of *C-H* and $N\text{-}H_2$ also increased at 1500 cm^{-1}. The power of $S\text{-}O_2$ bending, similar to the amount of *P(VSA.Na),* increased at 1700 cm^{-1}. Furthermore, the *O-H* bending intensity showed an increase at 1200 cm^{-1}, as depicted in Fig1.

In *P(VSA.Na),* SO_2 bending created the peak intensities at 1050 cm^{-1}. Developed bending at 1300 cm^{-1} was because of *OH* bending, and *OH* stretching peaked at 3500 cm^{-1}. An increase in the *P(VSA.Na)* amount can make prominent peaks. *FT-IR* spectra were obtained after heating the polymer at 170°C for 30, 60, and 180 minutes. All obtained spectra were the same with no difference (Fig.1-2).

The bending vibrations of *OH*, SO_2, and NH_2 were observed at 1300 cm^{-1}, 1150 cm^{-1}, and 1450 cm^{-1}, respectively. The interaction between *P(AlAm.HCl)* and *P(VSA.Na) IPC* (Fig. 1) resulted in a displacement towards longer wavelengths. Although the *FT-IR* spectrum of *P(AlAm.HCl)* and *P(VSA)* has been examined and documented, it is not included in this particular listing.

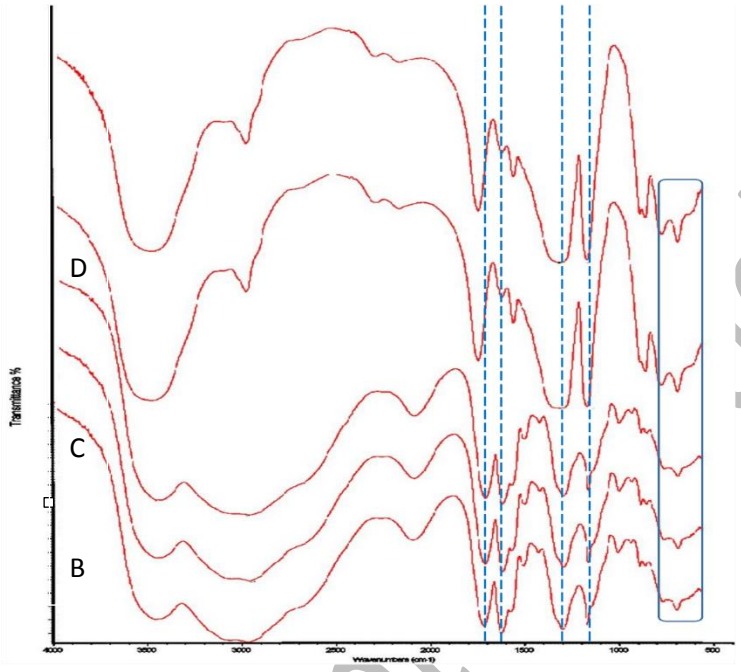

Figure 1. *FT-IR* spectra of *P(AlAm.HCl)* and *P(VSA.Na) IPCs*, prepared in different mole ratios of feed compositions **a)** (1:1), **b)** (1:0.5), **c)** (1:0.25), **d)** (0.5:1), **e)** (0.25:1)

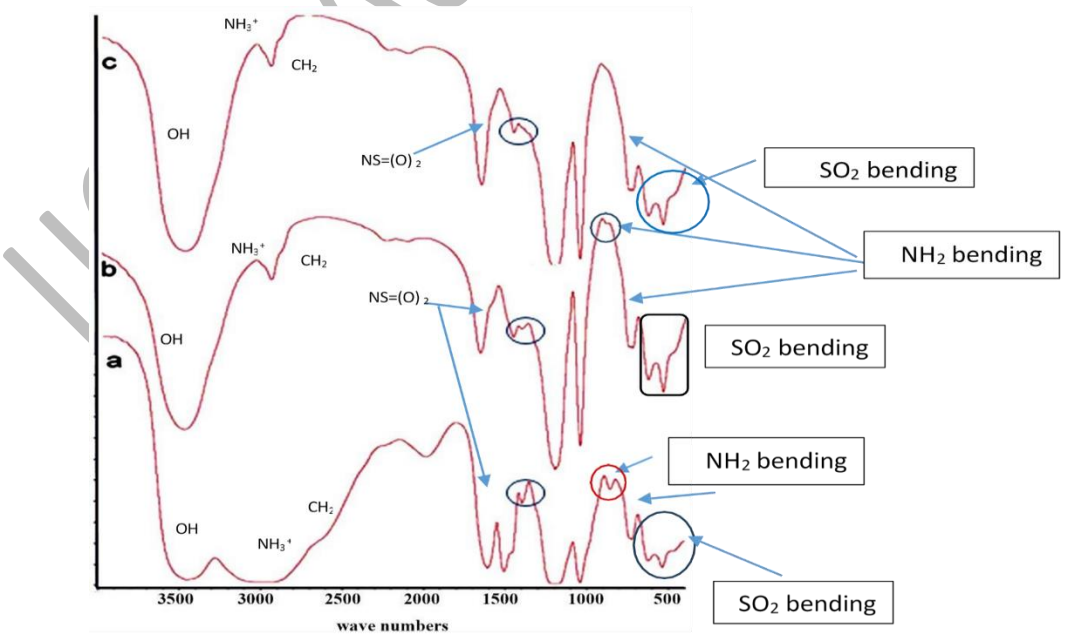

Figure 2. *FT-IR* spectra of *P(AlAm)* and *P(VSA)* in different mole ratio of feed composition **a)** (1:1), **b)** (1:0.25), **c)** (0.25:1)

The mixture of *P(AlAm.HCl)+P(VSA.Na)* was subjected to a process to prepare *IPC* with *P(AlAm)* and P(VSA). This involved the removal of HCl from the mixture, resulting in the conversion of *P(AlAm.HCl)* to *P(VSA)* and the dissolution of polymers in water. Subsequently, *P(VSA)* was added to *P(AlAm)*, leading to the occurrence of a white precipitate. The precipitate was then dried in a vacuum at 50ºC for 24 hours. To analyze the composition of the resulting *IPC*, *FT-IR* spectra were obtained and are presented in Figure 3. Notably, the stretching of NH_2 was observed at 3100 cm^{-1}, indicating a (1:1) mole ratio of feed composition. Sulfoamidization occurred at 1700 cm^{-1} in (0.25: 1) and (1:0.25) mole ratios of feed composition. Weak NH_2 bending was shown at 900 and 1400 cm^{-1}. *IPCs* were prepared at different mole ratios of feed composition and were heated at 170°C for 30, 60, and 180 minutes. *FT-IR* spectra of *IPCs* are shown in Figure 3. The sulfonamide group is observed at 1690-1750 cm^{-1}, secondary to the temperature effect in *FT-IR* spectra. Increased peak intensities observed at 1690-1750 cm^{-1} support the sulfonamide bond.

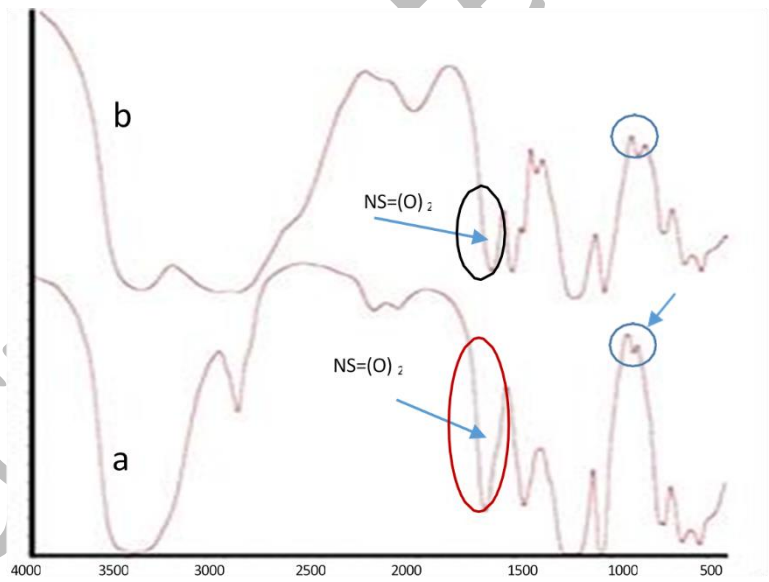

Figure 3. *FT-IR* spectra of *P(AlAm)+ P(VSA) IPC* at **a)** 170ºC, **b)** room temperature

Table1: *FT-IR* spectra of *P(AlAm) + P(VSA)* at room temperature and at170 ºC

Bands *(cm^{-1})*	**Assignments**
3500	O-H stretch
3000	N-H_2 stretch
2950	C-H_2 stretch
1700	NH-SO_2 in AlAm and VSA
1500	N-H bending in AlAm
1400	N-H_2 bending
1200	O-H bending
1000	C-H bending
500-700	N-H and S-O_2 bending

Figure 3 shows the *FT-IR* spectra analysis at 170℃ and 25℃. The shoulder bending of NH_2 disappeared at 1400 cm^{-1} in 25℃ but increased at 170 ℃. The increasing peak intensity indicates sulfamidization at 1690-1750 cm^{-1}.

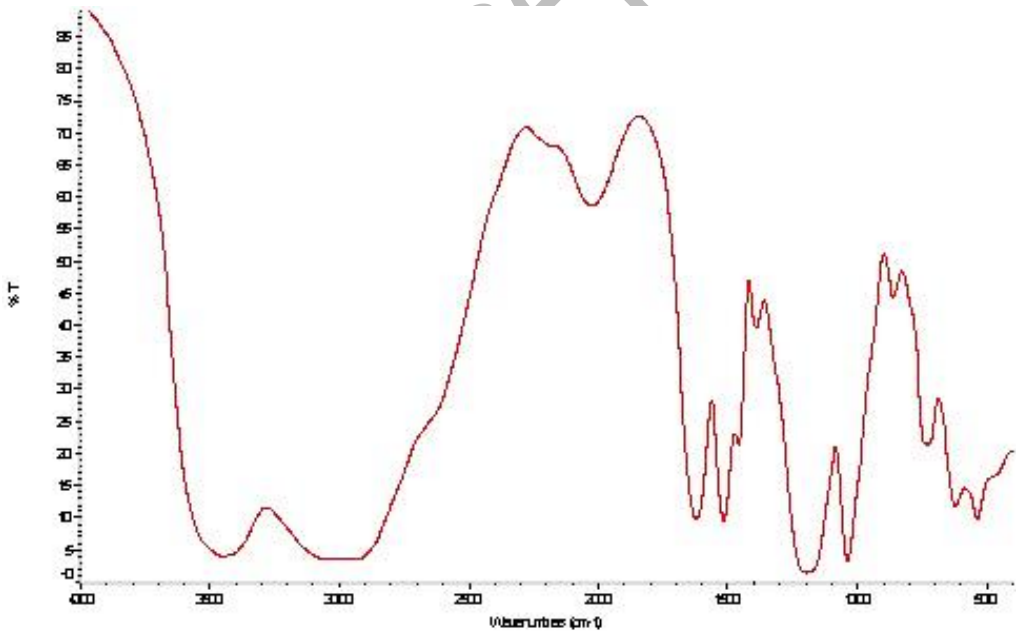

Figure 4. *FT-IR* spectrum of *IPC* of *(AlAm.HCl) + P(VSA.Na)* in (1:1) mole ratio of feed composition at room temperature

By taking the (1:1) mole ratio of feed composition of the *P(VSA.Na)+ P(AlAm.HCl) IPC*, no variation was shown at room temperature and 170℃. This is the hindrance of the sulfonamide reaction in the presence of *NaCl* (Fig. 4)

Investigation of IPC Structure by NMR

Different mole ratios of *P(AlAm)* and *P(VSA.Na)* were used to prepare *IPCs* in the feed composition. The *NMR* spectra of the *IPCs* confirmed the formation of weak structure complexes. *P(AlAm)* and *P(VSA.Na)* were easily dissolved in deionized water *(D_2O)*. The structural behavior of the *IPCs* was investigated through *^{1}H-NMR* measurements of the homo-polymer, as shown in Figure 5-6. In the *^{1}H-NMR* spectrum of *P(AlAm.HCl)*, the presence of the *CH_2* peak at one ppm indicated degradative chain transfer on the main chain. The *CH_2* peak also exhibited a rise due to main chain polymerization at 1.2-1.7 *ppm*. The *CH* peak, observed at 1.8-2.2 *ppm*, was attributed to polymerization. The height of the *CH_2* proton at 2.8-3.3 *ppm* indicated side chain transfer, while the *CH_2* peak at 3.4-3.7 *ppm* was due to degradative chain transfer on the side chain. Figure 6b depicted the *^{1}H-NMR* spectrum of *P(AlAm)*, which showed the presence of the *CH_2* peak (0.99-1.4 ppm), *CH* peak (1.4-1.7 ppm), *CH_2* peak on the side chain (2.4-2.8 *ppm*), *NH_2* peak (3.4-3.8 *ppm*), and *CH_2* peak due to degradative chain transfer on the side chain (2.1-2.2 *ppm*). Upon acid removal, the *CH_2* group of the primary chain shifted to 0.98 *ppm*, *CH* shifted to 1.4 *ppm*, *CH_2* on the side chain shifted to 2.4 *ppm*, and the free amine group shifted to 3.4 *ppm*. These shift values indicated the removal of acid from the *P(AlAm.HCl)* complex. [25]

ʊ *^{1}H-NMR* 400*MHZ* *(D_2O)*: 4.2-2.9 *(CH_2CHSO_3Na)*, polymer backbone, 2.9-1.4 *(CH_2CHSO_3Na)*, polymer backbone, 1.45 *(2H, OCH_2CH_3)*, 1.45-1.2 *(3H, $CHCH_3$)*. [26-27]

ʊ *^{13}C-NMR* 400 *MHZ* *(D_2O)*: 38-28 *ppm* *(CH_2CHSO_3Na)*, polymer backbone, 60-50 *ppm* *(CH_2CHSO_3Na)*, polymer backbone. [26-27]

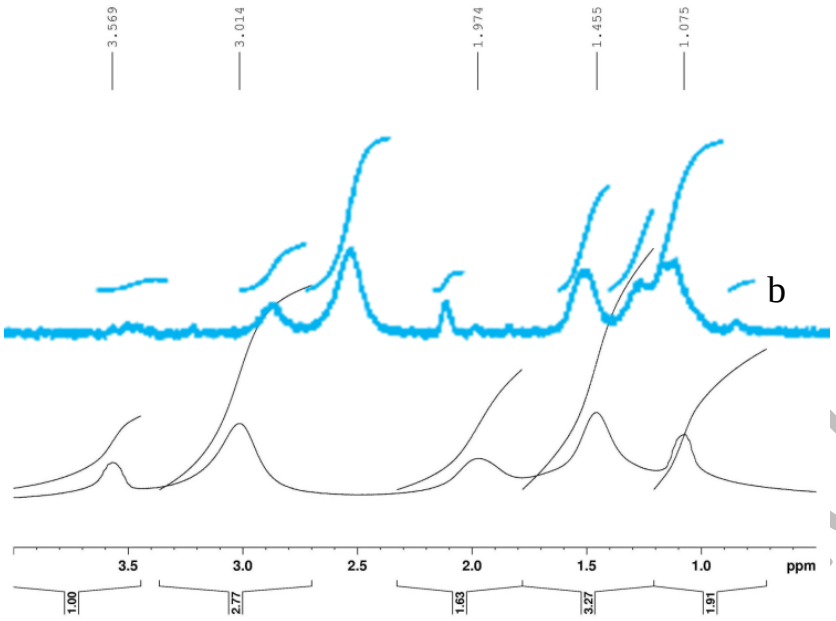

Figure 5. The *[1]H-NMR* spectrum of **a)** *P(AlAm.HCl)*, **b)** *P(AlAm)*

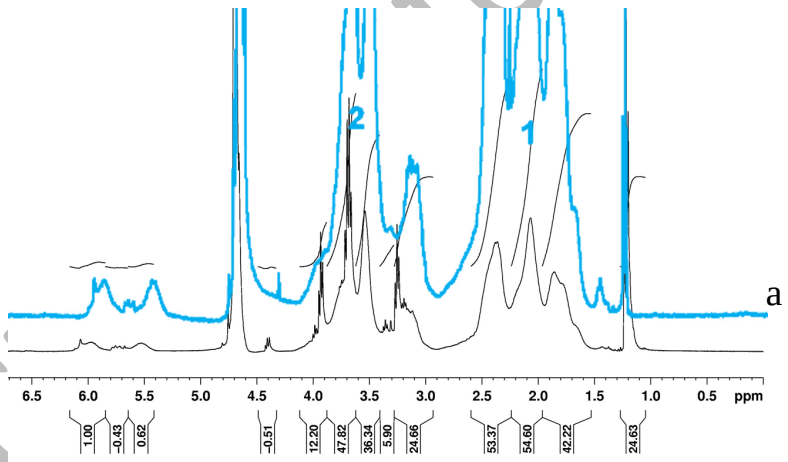

Figure 6. The *[1]H-NMR* spectrum of **a)** *P(VSA)*, **b)** *P(VSA.Na)*

The complexation between *P(AlAm)+P(VSA)* was evaluated by the *[1]H-NMR* spectroscopy. The *IPCs* of *P(AlAm)+P(VSA)* with (1:1), (1:0.25), and (0.25:1) mole ratios on feed composition are shown in Fig 7. The chemical shifts are compatible with the *IPC, [P(AlAm)+ P(VSA)]* shift to a high field compared to the pure homopolymers of *P(AlAm)* and *P(VSA)* secondary to the *IPCs* complexation. The *[1]H-NMR* scope of the *(AlAm.HCl), P(AlAm), P(VSA),* and *P(VSA.Na)* homopolymers are shown in Fig. 5-6.

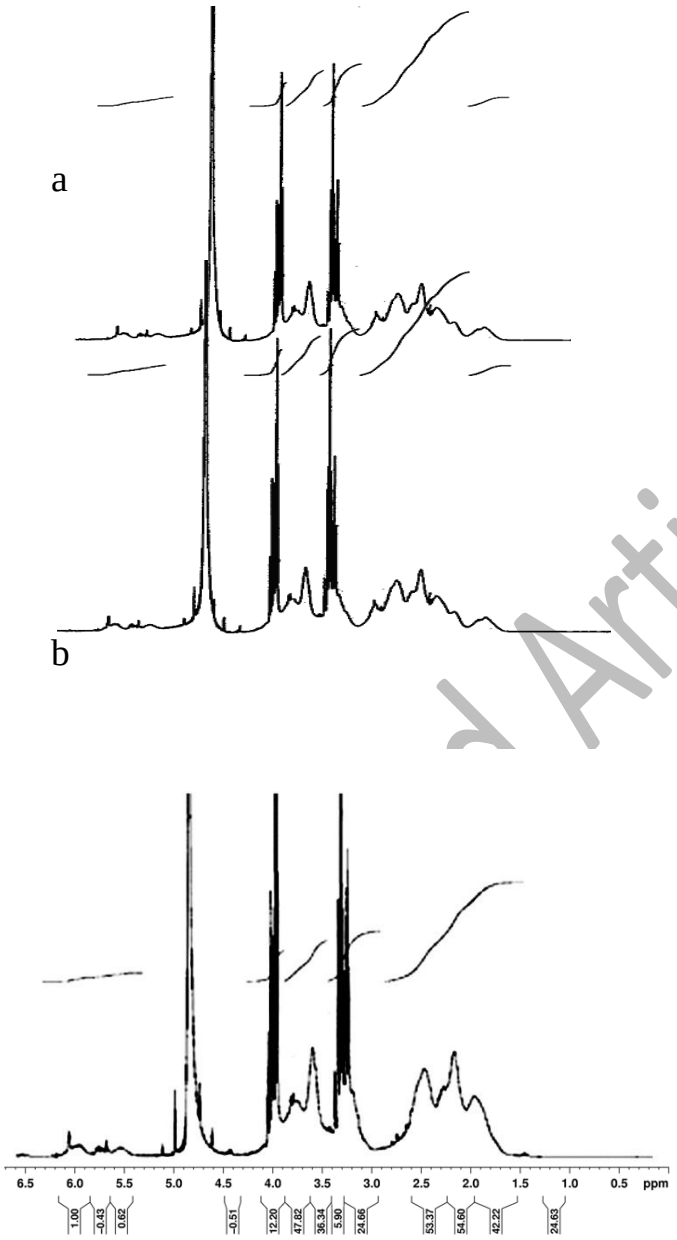

Figure 7. a) *^{1}H-NMR* prepared (1:1) mole ratio of *P(AlAm)+P(VSA)* on a repeating unit basis, **b)** (1:0.25) mole ratio of *P(AlAm)+P(VSA)* on a repeating unit basis, **c)** (0.25:1) mole ratios of *P(AlAm)+P(VSA)* on a repeating unit basis.

Investigation of IPC by XRD and SEM

XRD and SEM investigation of P(AlAm.HCl)+P (VSA.Na)

The *X*-ray diffraction *(XRD)* patterns of both homo- and copolymers were obtained using a Rigaku *D/MAX*-2200 diffractometer. Despite the amorphous nature of the structures, the *XRD* patterns of *P(AlAm)* exhibited sharp and well-defined peaks. This phenomenon can be attributed to the removal of *HCl* from *P(AlAm)* and the presence of *NaCl* in the medium, which

prompted the conversion of the structure into a more standardized form. (Fig. 8). The *XRD* patterns of *P(AlAm.HCl)* and *P(VSA.Na)* polymers exhibited well-defined peaks, which were attributed to the presence of *NaCl* in the medium and the considerable degree of complexation. These sharp peaks were observed across various mole ratios utilized in the preparation of the compositions. (Fig. 9). The *XRD* profiles of the *IPCs* consisting of acidless *P(AlAm)* and exhibiting a highly weak complexation and amorphous structure were examined. (Fig. 11)

Upon removal of the acid, the formation of *P(VSA) IPC* from *P(AlAm)* occurred, resulting in an observed balance reaction. This reaction was subsequently observed in *IPCs*. To determine the degree of crystallinity, it is necessary to separate the scattering from the crystalline and amorphous components in the diffraction pattern. The *XRD* patterns of *P(AlAm.HCl)* and *P(VSA.Na)* were recorded separately, revealing the presence of only amorphous peaks. To calculate the crystallinity of the *P(AlAm.HCl)* and *P(VSA.Na) IPCs*, the following equations were utilized. The degree of crystallinity *(Xc)* is determined by the ratio of the integrated crystalline scattering to the total distribution, encompassing both crystalline and amorphous components, as expressed in *Eq. (1)*.

Eq. (1) $x_C = \int_0^\infty s^2 I_c(s)\, ds \,/\, \int_0^\infty s^2 I(s)\, ds$

The magnitude of the reciprocal-lattice vector, denoted as *s*, can be calculated using the formula $s = (2\sin q)/l$, where *q* represents the one-half angle deviation of diffracted rays from incident *X*-rays, and *l* represents the wavelength. The intensities of coherent *X*-ray scattering from both the crystalline and amorphous regions are represented by *I(s)* and *Ic(s)*, respectively. Additionally, *Ic(s)* specifically refers to the intensity of the crystalline region in the polymer sample. The X-ray diffraction *(XRD)* measurements were used to determine the basal spacing *(d001)* of the interpenetrating polymer composites *(IPCs)*. The *XRD* patterns, which depict the crystallinity of the power complexation process, are presented in Figures 9-12. All the *XRD* parameters obtained from the analysis are summarized in Table 2. Additionally, the *X*-ray diffraction diagrams of the *P(AlAm.HCl)+P(AlAm)* powders can be observed in Figures 8-9.

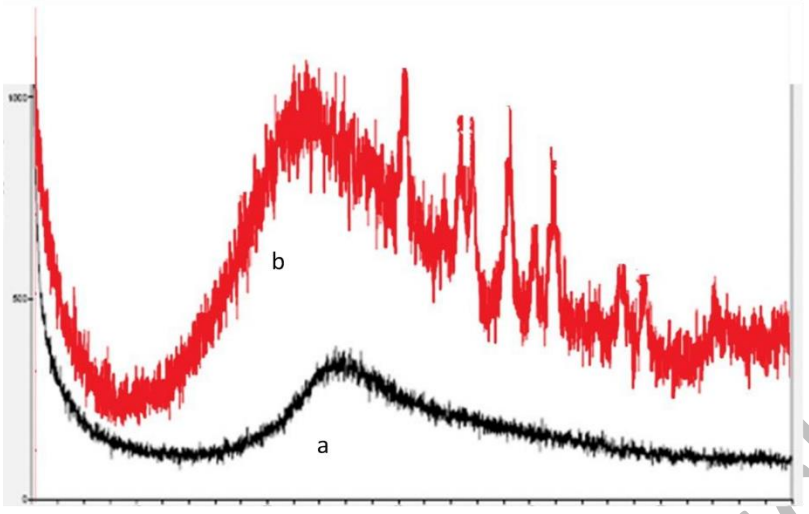

Figure 8. *XRD* pattern of **a)** *P(AlAm.HCl)* and **b)** *P(AlAm)*

It is observed in Table 2 that the *P(AlAm.HCl)* amount is low, while the crystallinity of the *IPC* (0.25:1) mole ratio of a repeating unit is high. It means the most potent complexation was obtained.

Table 2. XRD parameters and crystallinity of P(AlAm.HCl)+P(VSA.Na) IPCs

P(AlAm.HCl)+P(VSA.Na) **Mole ratio**	***2θ*** ***(°)***	**Intensity (Counts)**	**Peak area (*S*)** S_a	S_c	χ_c ***(%)***
(1:1)	31.6	875	3935	2776	41.4
(1:0.5)	32.082	1105	3437	2676	43.8
(1:0.25)	31.841	744	3864	2663	40.8
(0.5:1)	31.841	1620	4623	3854	45.5
(0.25:1)	31.738	2696	4808	4715	49.5

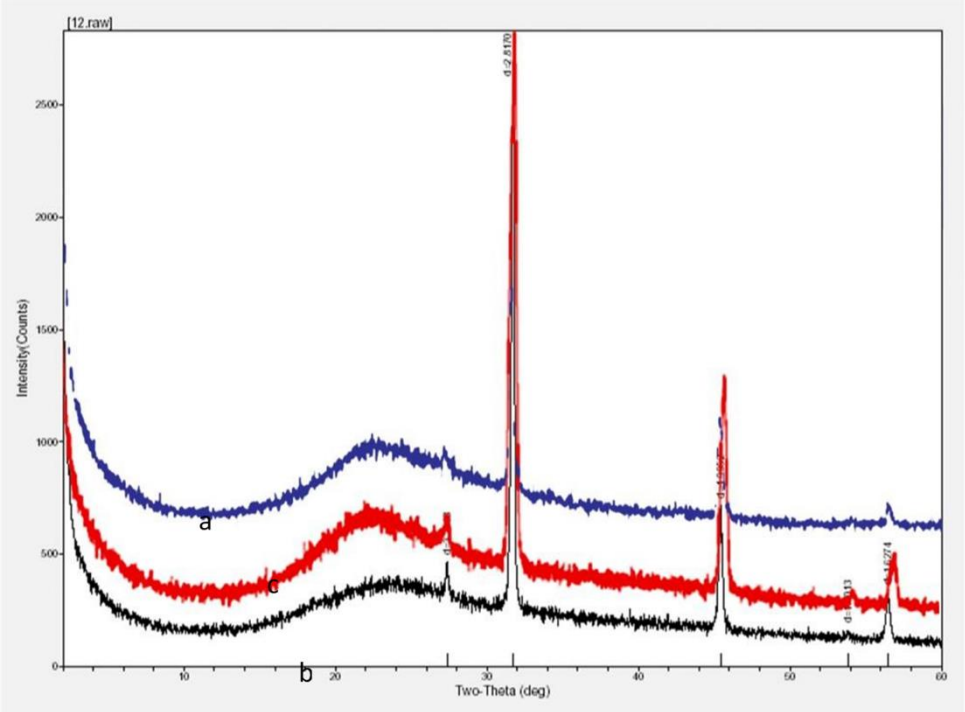

Figure 9. *XRD* patterns of *IPCs* between *P(AlAm.HCl)* and *P(VSA.Na)* **a)** (1:1), **b)** (0.5:1), **c)** (0.25:1) mole ratios on a repeating unit

For the investigation of morphology behavior, we used *SEM*. The morphology of *IPC* in (0.25:1) mole ratio of a repeating unit *P(AlAm.HCl)+P(VSA.Na)* shows the *NaCl* crystal on the *IPC*. (Fig10) It was the most potent *IPC* that was confirmed by *XRD* analysis.

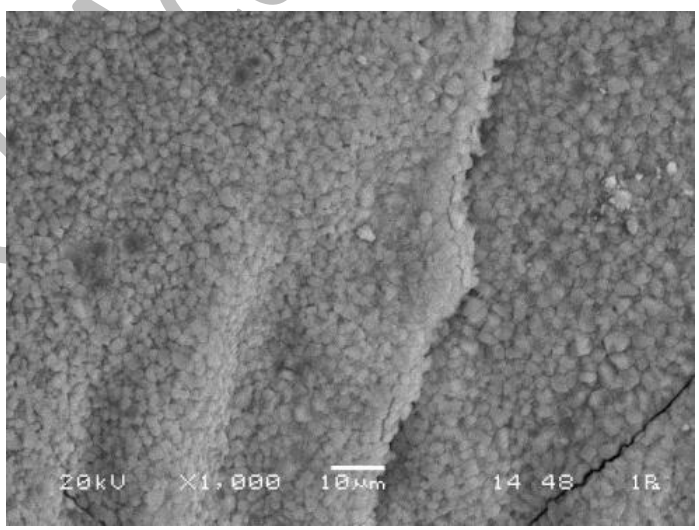

Figure 10. *SEM* micrograph of *IPCs* between *P(AlAm.HCl)* and *P(VSA.Na)* on (0.25:1) mole ratio on a repeating unit

Fig. 11 presents the preparation of *P(AlAm.HCl)+P(VSA.Na) IPCs* through the physical mixture method at various mole ratios, with the monomer unit serving as the reference point.

The *XRD* patterns were obtained for the five different compositions of *P(AlAm.HCl)+P(VSA.Na) IPCs*. Notably, the *XRD* patterns exhibited prominent peaks corresponding to *NaCl*, indicating the formation of a robust complexation resulting from the *NaCl* formation.

Investigation of P(AlAm)+P(VSA.Na) IPCs by XRD

XRD patterns of *P(AlAm)+P(VSA.Na) IPCs* had amorphous peaks.

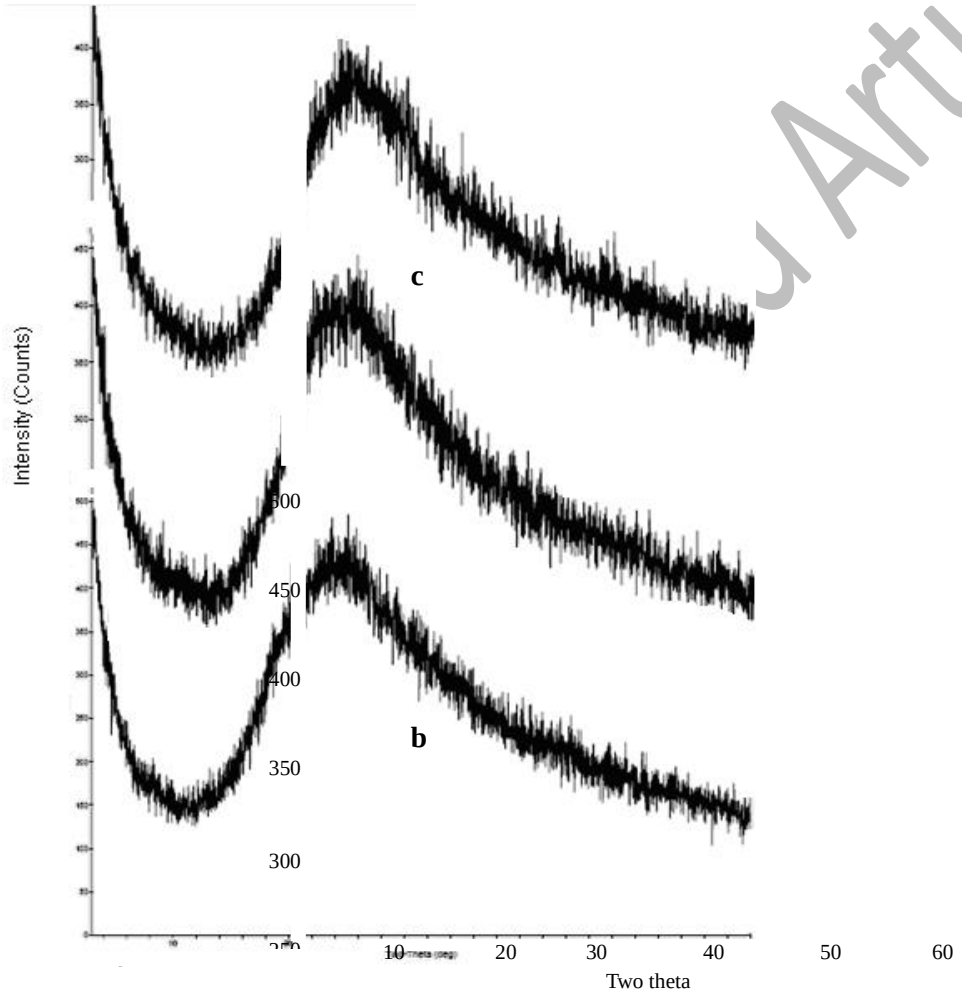

Figure 11. *XRD* patterns of **a)** (1:0.25), **b)** (1:0.5), **c)** (1:1) mole ratio of feed compositions *P(AlAm)+P(VSA.Na) IPCs*

In accordance with Figure 11, the removal of *HCl* from the strong complexation resulted in a decrease in crystallinity, leading to the complete amorphous nature of the structures. [25-27]

Investigation of Thermal Behavior of *P(AlAm.HCl+P(VSA.Na) IPCs* by *TGA*

The *TGA* technique was employed to examine the thermal stability of *P(AlAm)* and *P(AlAm.HCl)* to investigate their behavior under varying temperatures. The thermal properties of *P(AlAm.HCl)* and *P(AlAm)* are illustrated in Fig 12a and Fig 12b, respectively. These figures provide valuable insights into the thermal characteristics of both compounds, shedding light on their stability and potential applications.

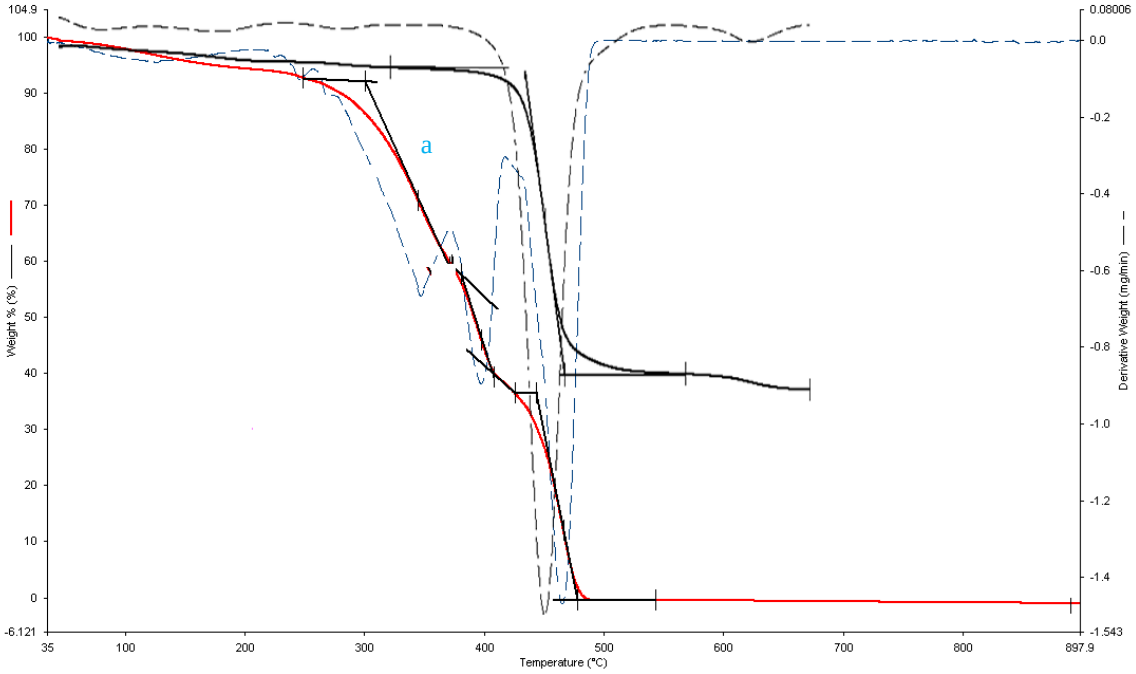

Figure 12. Thermal degradation of **a)** *P(AlAm.HCl)*, **b)** *P(AlAm)*

In Figure 12a, it can be observed that the thermal degradation of *P(AlAm.HCl)* takes place in three distinct steps. The initial step occurs between 300ºC and 370ºC, during which *HCl* is removed from the base polymer. The second step, which takes place from 380ºC to 408ºC, corresponds to the removal of the amine groups. The weight loss percentage observed during these two steps corresponds to the weight of *HCl* and the amine groups. The third step begins at 444ºC and concludes at 478ºC, during which all of the polymers decompose and transform into carbon black. [25]

On the other hand, the thermal behavior of *P(AlAm)* demonstrates a strong thermal property, as depicted in Figure 12b. This property becomes evident at approximately 440ºC. The weight loss of the polymer occurs in a single step, starting at 444ºC and ending at 479ºC. Interestingly, a significant portion of the polymer, approximately 45%, remains thermally stable even at temperatures as high as 700ºC. This enhanced stability at elevated temperatures can be attributed to the formation of ring structures along the polymer chain. These cyclic structures exhibit stability during the thermal degradation process of *P(AlAm)* under a nitrogen atmosphere, similar to the thermal behavior observed in poly(acrylonitrile). The vulnerability of the polymer to thermal degradation is caused by the attachment of *HCl* molecules to each amine group. [25]

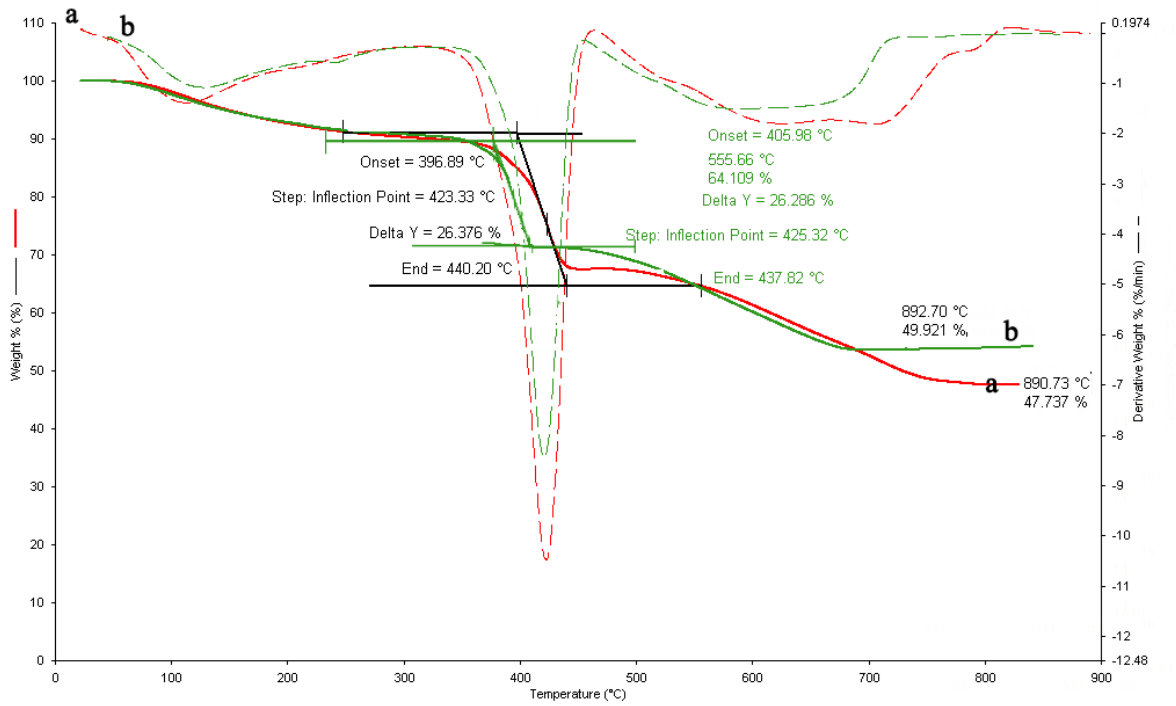

Figure 13. Thermal degradation of **a)** *P(VSA)*, **b)** *P(VSA.Na)*

The degradation of *P(VSA)* through thermal means follows a 4-step process, with the highest temperature of degradation observed at 420 ºC. The initial step, occurring between 90 and 200 ºC, is likely attributed to the presence of retained water. The actual degradation takes place in the second step, commencing at 300ºC and extending until 450ºC. During this stage, approximately 30% of the polymer undergoes degradation. Moving on to the third stage spans from 450 to 650ºC. At 600ºC, the sample remains non-volatile, while a 5% mass loss is observed at 200ºC. When subjected to acid degradation, a significant amount of foam is generated. The fourth and final step initiates at 670ºC and concludes at 780ºC, with 50% of the

polymer undergoing degradation. Remarkably, even at 900 ºC, 47% of the polymer remains intact, as depicted in Figure 13a. [26]

The degradation of *P(VSA.Na)* can be observed through three distinct processes. The initial process takes place within the temperature range of 100 to 300 ºC, resulting in a degradation of 10% of the polymer. The most significant degradation of the polymer chains occurs during the second process, which spans from 380 to 500ºC, leading to a degradation of 40% of the polymer. The final step of the degradation process commences at temperatures ranging from 500 to 750ºC, leaving behind 50% of the polymer. When the degradation occurs in a nitrogen environment, the foam exhibits the formation of a mineral residue and volumetric expansion at 350ºC, as evidenced by *TGA* analysis (Fig 13b). [26] Furthermore, the thermal properties of the *P(AlAm. HCl)* and *P(VSA)* and *P(AlAm. HCl)+P(VSA) IPC* were investigated.

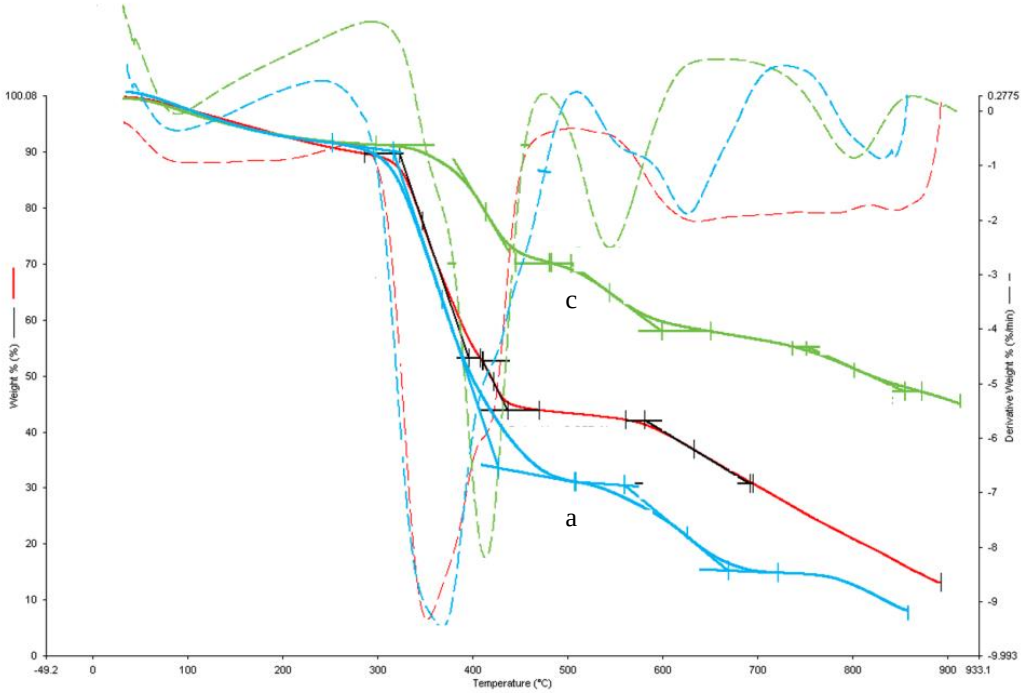

Figure 14. Thermal degradation of *P(AlAm.HCl)+P(VSA.Na) IPCs* prepared from **a)** (1:1), **b)** (1:0.25), **c)** (0.25:1) mole ratio of feed composition

Figure 14a illustrates the thermal degradation of *P(AlAm.HCl)+P(VSA.Na)* in a 1:1 mole ratio of feed composition. The degradation process occurs in three steps, with the maximum degradation temperature observed at 347ºC. The first step begins at 323ºC and continues until 396ºC, resulting in a 50% weight loss. Specifically, the degradation of *P(AlAm.HCl)* takes place at around 300ºC, as shown in Figure 15. The second step occurs between 411ºC and 436ºC, involving the degradation of *P(VSA.Na).* Finally, the third step spans from 580ºC to 894ºC. [25-27]

In Figure 14b, the thermal degradation of *P(AlAm.HCl)+P(VSA.Na) IPC* in a (1:0.25) mole ratio of feed composition is presented. This degradation process follows a two-step phase, with the maximum degradation temperature observed at 380ºC. It initiates at approximately 327ºC and concludes at around 443ºC, resulting in a weight loss of approximately 60%. During this step, the degradation of *P(AlAm.HCl)* occurs. The second process commences at 582ºC and terminates at approximately 694ºC, involving the degradation of *P(VSA.Na)*. [25-27]

Figure 14c displays the thermal degradation of the (0.25:1) *IPC*. This degradation process follows a three-step pattern, with the highest degradation temperature observed at approximately 400ºC. It commences around 360ºC and concludes at approximately 432ºC. Both *P(AlAm.HCl)* and *P(VSA.Na)* undergo degradation during this step. The second step begins at around 489ºC and finishes at approximately 584ºC. Finally, the third step occurs at 732ºC and terminates at around 835ºC. [25-27]

When comparing the thermal degradation of five *IPC* polymers with different mole ratios of monomers inter-polymer complex, the (0.25:1) *IPC, P(AlAm.HCl)+P(VSA.Na)* in different mole ratios of feed composition, emerges as the most significant. This is confirmed by *XRD* patterns, which can be further illustrated in Tables 1-5.

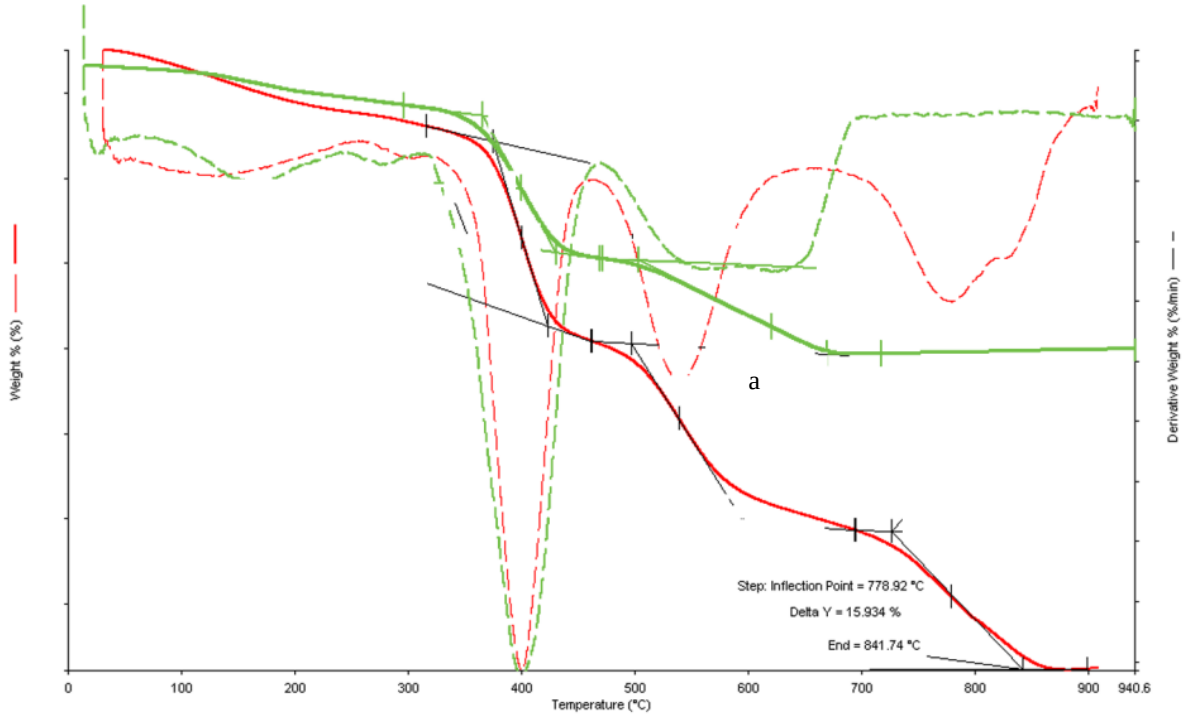

Figure 15. Thermal degradation of **a)** *P(AlAm)+P(VSA.Na) IPC* prepared from (1:1) mole ratio of feed composition, **b)** *P(AlAm)+P(VSA) IPC* prepared from (1:1) mole ratio of feed composition

In Figure 15a, the degradation of *IPCs* due to thermal factors occurs through a three-step process, reaching its peak degradation temperature at approximately 400ºC. The initial step of degradation takes place within the temperature range of 374ºC to 423ºC. Subsequently, the second step commences between 496ºC and approximately 595ºC. Finally, the third step initiates at temperatures ranging from 726ºC to 841ºC. [25-27]

In contrast, Figure 15b illustrates a distinct thermal degradation pattern for *IPCs*, characterized by a two-step process. The highest temperature at which degradation occurs is measured at 398ºC. The initial step of degradation takes place within the temperature range of 362ºC to 424ºC, while the subsequent step commences between 493ºC and 649ºC. Figure 15a is an outline to compare the two *IPCs* that are shown in Fig (14a,14b), which show sodium presence at 900ºC leads to nearly 53.6% of substance remaining. With sodium in Fig.14a, the pH of the blend *IPC* is changed, and the strength of the hydrogen bonds decreases. However, in Fig 14b, a strong hydrogen bond is formed between two polymers and the initial degradation temperature increases to 374ºC. At 900ºC, all of the *IPC* polymers are degraded. Tables 6-7 denote the above-mentioned data. [25-27]

Table 3. Data of TGA for IPC in (1:1) P(AlAm.HCl), P(VSA.Na)

	Onset	Inflection point	End
Step 1	321°C	344°C	396°C
Step 2	411°C	421°C	436°C
Step 3	580°C	633°C	892°C 900°C (%13.12 remained)

Table 4. Data of TGA for IPC in (1:0.5) P(AlAm.HCl), P(VSA.Na)

	Onset	Inflection point	End
Step 1	323°C	374°C	416°C
Step 2	422°C	456°C	487°C
Step 3			900°C (%15.22 remained)

Table 5. Data of TGA for IPC in (1:0.25) P(AlAm.HCl), P(VSA.Na)

	Onset	Inflection point	End
Step 1	317°C	381°C	443°C
Step 2	580°C	551°C	697°C
Step 3			900°C (%3.09 remained)

Table 6. Data of TGA for IPC in (0.5:1) P(AlAm.HCl), P(VSA.Na)

	Onset	Inflection point	End
Step 1	327°C	353°C	370°C
Step 2	374°C	407°C	446°C
Step 3	485°C	519°C	575.5 900°C (%16.3 remained)

Table 7. Data of TGA for IPC in (0.25:1) P(AlAm.HCl), P(VSA.Na)

	Onset	Inflection point	End
Step 1	360°C	401°C	433°C
Step 2	489.5°C	530°C	584°C
Step 3	733°C	782°C	834°C 900°C (%33.5 remained)

Table 8. Data of TGA for IPC in (1:1) P(AlAm), P(VSA)

	Onset	Inflection point	End
Step 1	374°C	400°C	423°C
Step 2	496°C	538°C	595°C
Step 3	726°C	779°C	841°C 900 °C(%0 remained)

Table 9. Data of TGA for IPC in (1:1) P(AlAm), P(VSA.Na)

	Onset	Inflection point	End
Step 1	362°C	395°C	424°C
Step 2	493°C	604°C	649°C
Step 3			900°C(%53.6 remained)

Conclusion:

Producing layer-by-layer films in the industry, modification of *DNA* in biology, and preparation of Nano gel and Microgels in drug delivery systems are among the most essential applications of *IPCs*. We used *P(AlAm.HCl)* and *P(VSA.Na)*, cationic and anionic polymers, to achieve *IPCs'* most potent complexation properties. We synthesized the polymers using the free radical polymerization method in previous studies. A mixture was prepared with different mole ratios of feed composition to reach the powerful complex. *XRD* and *TGA* investigated the prepared *IPC* to assess the complex power. Strong *IPCs* were formed in the mole ratio (0.25:1) in feed compositions confirmed by *XRD* and *TGA*. *FT-IR* Spectroscopy was used for the investigation of *IPC's* structural behavior. The *XRD* patterns revealed that the *IPCs* exhibited the highest level of crystallinity at a concentration of 50%. In addition, *P(AlAm)* and *P(VSA)* interpenetrating polymer complexes *(IPCs)* were synthesized through the removal of *HCl* from *P(AlAm.HCl)* and the conversion of *P(VSA.Na)* to *P(VSA).* Both polymers exhibited solubility in water. The presence of NH_2 stretching at 3100 cm^{-1} was observed in mole ratios of 1:1, while sulfamidization was observed at 1700 cm^{-1} in mole ratios of 0.25:1 and 1:0.25. The *FT-IR* spectra obtained from samples prepared at various mole ratios of feed composition and kept at 170°C for 180 minutes (similar to 30 minutes and 60 minutes) showed the presence of the

sulfonamide group, which can be attributed to the influence of temperature. *NMR* spectra confirmed the existence of a weak complexation in the different mole ratios of feed composition. *P(AlAm)* and *P(VSA.Na) IPCs* were synthesized based on different mole ratios on a repeating unit basis and were easily dissolved. The structural analysis was conducted using *NMR* spectroscopy. The *XRD* patterns of the *P(VSA) IPCs* were formed by the acidless form of *P(AlAm).* Weak complexation and amorphous structure were found between *P(VSA)* and *P(AlAm).* Microgel and Nano gel production to apply in the pharmaceutical industry and drug delivery systems is a future research horizon. Using different environmental conditions such as temperature, *pH*, and ionic effect to prepare potent *IPCs* is the other scope of our studies.

Conflict of Interest:

There is nothing to declare.

Financial funding:

There are no sources of financial funding and support.

References:

1) Radha K.P., Selvasekarapandian S., Karthikeyan S., Hema M., Sanjeeviraja C., Synthesis and impedance analysis of proton-conducting polymer electrolyte PVA: NH4FIonics, *Ionic*,19:1437-47 (2013). https://doi.org/10.1007/s11581-013-0866-5

2) Arunkumar R., Babu Ravi Shanker M., Usha Rani M., Kalainathan S.J., Effect of PBMA on PVC-based polymer IPC electrolytes, *Appl. Polym. Sci.* , 134, 44939-50 (2017). https://doi.org/10.1002/app.44939

3) Angulakshmi N., ManuelStephan, A., Electrochem.Acta, A., Electrospun Trilayer Polymeric Membranes as Separator for Lithium, *ion Batteries*, 127, 167 (2014). https://doi.org/10.1016/j.electacta.2014.01.162

4) Liew C.W., Ramesh S., Arof A.K., Characterization of ionic liquid added poly(vinyl alcohol)-based proton conducting polymer electrolytes and electrochemical studies on the supercapacitors, *Int. J. Hydro. Energy*, 40, 852-862 (2015). https://doi.org/10.1016/j.ijhydene.2014.09.160

5) Evecan D., Gurcuoglu O., Zayim E.O., Electrochromic device application of tungsten oxide film with polymer electrolytes, *Microelectr. Eng.* 128, 42 (2014). https://doi.org/10.1016/j.mee.2014.05.031

6) Cui Y., Zhang J., Wang P., Zhang X., Zheng J., Sun Q., Feng J., Yuejin Z., LiTFSI as a plastic salt in the quasi-solid state polymer electrolyte for dye-sensitized solar, *Electrochim. Acta*, 74, 194 (2012). https://doi.org/10.1016/j.crci.2012.10.015cells

7) Mittal V., "Functional Polymer IPC Synthesis, Properties, and Performance" *Functional Polymer Blends*; CRC Publishers, London, (2012). https://doi.org/10.1201/b11799

8) Rhoo H.J., Kim H.T., Park J.K., Hwang T.S., Ionic conduction in plasticized PVCPMMA blend polymer electrolytes, *Electrochim. Acta*, 42, 1571 (1997). https://doi.org/10.1016/S0013-4686(96)00318-0

9) Rajendran S., Babu R., Sivakumar P.J., Optimization of PVC– PAN-based polymer electrolytes, *Appl. Polym. Sci.*, 113, 1651-6 (2009). https://doi.org/10.1002/app.30174

10) Yusuf S.N.F., Yusof S.Z., Kufian M.Z., Teo L.P., Preparation and electrical characterization of polymer electrolytes: A review, *Materials today proceeding*, 17(2): 446-458 (2019). https://doi.org/10.1016/j.matpr.2019.06.475

11) Kudaibergenov S.E., Nuraje N., Intra- and Interpolyelectrolyte Complexes of Polyampholytes, *Polymers*, 10(10):1146 (2018). https://doi.org/10.3390/polym10101146

12) Kabanov V.A., Zezin A.B., Soluble interpolymeric complexes as a new class of synthetic polyelectrolytes, *Pure Appl. Chem.*, 56(3): 343-354 (1984). https://doi.org/10.1351/pac198456030343

13) Wen Z.Y., Itoh T., Ichikawa Y., Kubo M., Yamamoto O., Blend-based polymer electrolytes of poly(ethylene oxide) and hyperbranched poly[bis(tri ethylene glycol)benzoate] with terminal acetyl groups, *Solid State Ionics*, 134(3-4): 281-289 (2000). https://doi.org/10.1016/S0167-2738(00)00707

14) Ma Y., Sun J., Shen J., Ion-Triggered Exfoliation of Layer-by-Layer Assembled Poly(acrylic acid)/Poly(allylamine hydrochloride) Films from Substrates: A Facile Way To Prepare Free-Standing Multilayer Films, *Chem. Mater.*, 19(21): 5058-5062 (2007). https://doi.org/10.1021/cm071260j

15) Zucolotto V., Ferreira M., Cordeiro M.R., Constantino C.J.L., Balogh D.T., Zanatta A.R., Moreira W.C., Oliveira O.N., Unusual interactions binding iron tetrasulfonated

phthalocyanine and poly (allylamine hydrochloride) in layer-by-layer films, *J. Phys. Chem. B*, 107(16): 3733-3737 (2003). https://doi.org/10.1021/jp027573d

16) Lourencüo J.M.C., Ribeiro P.A., Botelho do Rego A.M., Braz Fernandes F.M., Moutinho A.M.C., Raposo M., Counterions in Poly(allylamine hydrochloride) and Poly(styrene sulfonate) Layer-by-Layer Films, *Langmuir*, 20(19): 8103–8109 (2004). https://doi.org/10.1021/la049872v

17) Thünemann A.F., Polyelectrolyte–surfactant complexes (synthesis, structure and materials aspects, *Prog. Polym. Sci.*, 27(8): 1473-1572 (2002). https://doi.org/10.1016/S0079-6700(02)00017-5

18) Kötz J., Kosmella, S., Beitz, T., Self-assembled polyelectrolyte systems, *Prog. Polym. Sci.*, 26, 1199-1232 (2001). https://doi.org/10.1016/S0079-6700(01)00016-8

19) Bertrand P., Jonas A., Laschewsky A., Legras R., Ultrathin polymer coatings by complexation of polyelectrolytes at interfaces: Suitable materials, structure, and properties, *Macromol. Rapid Comm.*, 21(7): 319-348 (2000). https://doi.org/10.1002/(SICI)1521-3927(20000401)21:7<319::AID-MARC319>3.0.CO;2-7

20) Ober C.K., Wegner G., Polyelectrolyte-surfactant complexes in the solid state. Facile building blocks for self-organizing materials, *Advanced Materials*, 9(1):17-31(1997). https://doi.org/10.1002/adma.19970090104

21) Antonietti M., Burger C., Thünemann A., Polyelectrolyte-surfactant complexes: a new class of highly ordered polymer materials, *TIPC*, 5(8): 262-267 (1997). https://doi.org/10.1002/MASY.19961060103

22) Antonietti M., Thünemann A., Polyelectrolyte-lipid complexes as membrane mimetic systems, *Curr Opin Colloid Interface Sci.*, 1(5): 667-671(1996). https://doi.org/10.1016/S1359-0294(96)80106-3

23) Ponomarenko E.A., Tirrell D.A., MacKnight W.J., Self-Assembled Complexes of Synthetic Polypeptides and Oppositely Charged Low Molecular Weight Surfactants. Solid-State Properties, *Macromolecules*, 29(12): 4340-4345 (1996). https://doi.org/10.1021/ma951088h

24) Kioussis D.R., Kofinas P., Characterization of anion diffusion in polymer hydrogels used for wastewater remediation, *Polymer*, 46(22):9342-9347 (2005). https://doi.org/ 10.1016/j.polymer.2005.07.045

25) Sepehrianazar A., Güven O., Free radical polymerization of allylamine in different acidic media, *Polymers and Polymer Composites*, 30 (2022) https://doi.org/10.1177/09673911221103599

26) Sepehrianazar A., Güven O., Synthesis and characterization of poly(vinyl sulfonic acid) in different pH values, *Polym. Bull.*, 80(3):3005-20 (2023). https://doi.org/10.1007/s00289-022-04190-6

27) Sepehrianazar A., Güven O., Synthesis and characterization of (allylamine hydrochloride-vinyl sulfonic acid) copolymer and determination of monomer reactivity ratios, *J Polym Res*, 29: 330 (2022). https://doi.org/10.1007/s10965-022-03106-2

28) Izumrudov V.A., Binur K.M., and Kunnaz B.M., Polyelectrolyte multilayers: Preparation and applications, *Russian Chemical Reviews* 87(2):192 (2018) https://doi.org/10.1070/rcr4767

29) Kiechel M.A., "Post-processing of electrospun chitosan fibers", Office of Graduate Studies, Doctor of Philosophy theses, Drexel University, Philadelphia, PA, USA, (2013).

30) Kofinas P., Kioussis D.R., Reactive Phosphorus Removal from Aquaculture and Poultry Productions Systems Using Polymeric Hydrogels, *Environ. Sci. Technol.*, 37(2): 423-427 (2003). https://doi.org/ 10.1021/es025950u

31) Bingöl B., Meyer W.H., Wagner M., Wegner G., Synthesis, Microstructure, and Acidity of Poly(vinyl phosphonic acid), *Macromol. Rapid Commun.*, 27(20):1719-1724 (2006). https://doi.org/10.1002/marc.200600513

32) Gradzielski M., Hoffmann I., Polyelectrolyte-surfactant complexes (PESCs) composed of oppositely charged components, *Current Opinion in Colloid & Interface Science (COCIS)*, *35*:124-141 (2018). https://doi.org/10.1016/j.cocis.2018.01.017

33) Pzdnyakov A.S., Sekeretarev E.A., Emelyanov A.I, Prozorova G.F., Hydrophilic functional copolymers of 1-vinyl-1,24-triazole with vinyl sulfonic acid sodium salt, *Russ. Chem. Bull*. 66(12):2293-2297 (2017). https://doi.org/10.1007/s11172-017-2017-z

34) Oztop H., Akyildiz F., Saraydin D., Poly(acrylamide/vinyl sulfonic acid) hydrogel for invertase immobilization, *Microsc Res Tech*, 83(12):1487-1498 (2020). https://doi.org/ 10.1002/jemt.23542.